




Joint quantum estimation of loss and nonlinearity in driven-dissipative Kerr resonators

Muhammad Asjad ¹, Berihu Teklu ^{1,2} and Matteo G. A. Paris ^{3,4}

¹*Department of Applied Mathematics and Sciences, Khalifa University, 127788 Abu Dhabi, United Arab Emirates*

²*Center for Cyber-Physical Systems (C2PS), Khalifa University, 127788 Abu Dhabi, United Arab Emirates*

³*Quantum Mechanics Group & Quantum Technology Lab, Dipartimento di Fisica 'Aldo Pontremoli dell'Università degli studi di Milano, I-20133 Milan, Italy*

⁴*Istituto Nazionale di Fisica Nucleare - Sezione di Milano, I-20133 Milan, Italy*



(Received 10 December 2022; accepted 8 February 2023; published 17 March 2023)

We address multiparameter quantum estimation for coherently driven nonlinear Kerr resonators in the presence of loss. In particular, we consider the realistic situation in which the parameters of interest are the loss rate and the nonlinear coupling, whereas the amplitude of the coherent driving is known and externally tunable. Our results show that this driven-dissipative model is asymptotically classical, i.e., the Uhlmann curvature vanishes, and the two parameters may be jointly estimated without any additional noise of quantum origin. We also find that the ultimate bound to precision, as quantified by the quantum Fisher information (QFI), increases with the interaction time and the driving amplitude for both parameters. Finally, we investigate the performance of quadrature detection, and show that for both parameters the Fisher information oscillates in time, repeatedly approaching the corresponding QFI.

DOI: [10.1103/PhysRevResearch.5.013185](https://doi.org/10.1103/PhysRevResearch.5.013185)

I. INTRODUCTION

Quantum properties of radiation and matter may provide enhanced precision in metrological applications [1,2]. Indeed, quantum systems are notoriously fragile and very sensitive to perturbations, even to very weak perturbations, which makes them inherently precise sensors. Quantum probes have been exploited to improve sensitivity [3–9], and the resulting quantum technology represents a fundamental tool to improve metrological standards and increase precision of several characterization techniques ranging from stochastic noise [10–13] to material science [14–18], and from biology [19–23] to gravitational wave detection [24,25].

For a single parameter of interest, the performance of a quantum sensor may be characterized in terms of the quantum Fisher information (QFI), which bounds the achievable precision via the quantum Cramér-Rao bound (QCRB). On the other hand, in many realistic situations one is interested in the joint estimation of two or more parameters [26–36]. Besides, the multiparameter case has fundamental interest for studying compatibility problems involving the noncommutativity of quantum operations [37–40]. In turn, the impossibility of jointly measuring noncompatible quantum observables makes it theoretically impossible to reach the multiparameter version of the QCRB bound.

Quantum mechanical features of physical systems provide room for new sensing and computing technologies. Loss

and decoherence usually limit the performance of quantum-enhanced protocols, though an accurate manipulation and control of the internal and external degrees of freedom makes it possible to overcome and sometimes exploit loss and dissipation. In this framework, driven-dissipative systems are of particular interest for a wide range of fields, ranging from foundations to solid state physics [23,41–56]. In this kind of system, one may explore the joint estimation of loss and nonlinearity by tuning the external driving in order to achieve the optimal working regime, possibly exploiting the existence of a stationary solution. In particular, here we address the paradigmatic example of driven-dissipative Kerr resonator [57], which represents a sensitive probe due to its strongly nonlinear response [58–67]. We investigate situations where the parameters of interest are the strength of the Kerr nonlinearity χ and the rate of (one-photon) loss γ , which are estimated by probing the optical medium with suitable optical signals. We focus on the nonequilibrium dynamics of the Kerr resonator, where the driving competes with incoherent dissipation and coherent amplification [68–70], and seek for configurations where the joint estimation of loss and nonlinearity is possible without any additional noise of quantum origin, possibly enhancing the single-parameter sensitivity of the system. This also paves the way to study more involved situations, e.g., regimes where also two-photon loss may play a role.

The structure of the paper is as follows. In Sec. II A we introduce the model, and in Sec. II B we briefly review the basic tools of local multiparameter quantum estimation theory. Specifically, we outline the ultimate bounds to precision in the joint estimation of the driven-dissipative Kerr nonlinear resonator. In Sec. III, we illustrate and discuss our results: in Sec. III A we show results about the time evolution of the

Published by the American Physical Society under the terms of the [Creative Commons Attribution 4.0 International](https://creativecommons.org/licenses/by/4.0/) license. Further distribution of this work must maintain attribution to the author(s) and the published article's title, journal citation, and DOI.

quantum Fisher information matrix, and in Sec. III B we discuss the performance of homodyne detection in the estimation of the two parameters. Finally, Sec. IV closes the paper with some concluding remarks.

II. PRELIMINARIES

A. Driven-dissipative Kerr resonator

The system we study is a general model of a single driven-dissipative Kerr nonlinear resonator of frequency ω_c whose coherent dynamics is described by the Hamiltonian

$$H = -\Delta \hat{a}^\dagger \hat{a} + \frac{\chi}{2} \hat{a}^\dagger \hat{a}^\dagger \hat{a} \hat{a} - iF(\hat{a} - \hat{a}^\dagger), \quad (1)$$

in the rotating-wave approximation, where $\Delta = \omega_p - \omega_c$ is the pump-cavity detuning, F is the coherent drive strength, and χ is the Kerr nonlinearity. The operator \hat{a}^\dagger (\hat{a}) is creation (annihilation) operator of the resonator. We assume that the resonator is coupled to a zero-temperature bath. Therefore, the full dissipative dynamics of such a system is described by the Lindblad master equation

$$\frac{d}{dt} \hat{\rho} = -i[\hat{H}, \hat{\rho}] + \frac{\gamma}{2} \mathcal{D}[\hat{a}] \hat{\rho} \equiv \mathcal{L}_0 \hat{\rho}, \quad (2)$$

where $\mathcal{D}[\hat{X}] \hat{\rho} \equiv \hat{X} \hat{\rho} \hat{X}^\dagger - (1/2)(\hat{X}^\dagger \hat{X} \hat{\rho} + \hat{\rho} \hat{X}^\dagger \hat{X})$ is the usual Lindblad dissipative superoperator, and γ is the one-photon decay rate. Systems described by the Hamiltonian in Eq. (1) may be realized using several experimental platforms such as semiconductor microcavities [71–74], quantum circuits [75–77], and optomechanical setups [78,79]. As a matter of fact, there may be other forms of loss other than incoherent dissipation in driven-dissipative systems. However, we focus on systems where the dynamics is governed by Eq. (2) for their relevance in practical applications.

B. Multiparameter quantum estimation

The quantum Fisher information is the main tool of quantum sensing and metrology, as it quantifies the ultimate precision in estimating a parameter encoded onto a quantum state. In turn, it also serves to assess whether and how a certain quantum system may be exploited as a sensing device. Let us consider a scenario in which we are interested in estimating the value of a vector of parameters $\lambda = (\lambda_1, \lambda_2, \dots)$ encoded onto a quantum state

$$\rho(\lambda) = \sum_k p_k(\lambda) |\rho_k(\lambda)\rangle \langle p_k(\lambda)|. \quad (3)$$

The quantum Fisher information matrix (QFIM) is defined as

$$\mathcal{F}_{jk} = \frac{1}{2} \text{Tr}[\rho(\lambda) \{ \mathcal{L}_j, \mathcal{L}_k \}], \quad (4)$$

where $\{A, B\} = AB + BA$ denotes the anticommutator, and the operators $\mathcal{L}_j \equiv \mathcal{L}_{\lambda_j}$ are the so-called symmetric logarithmic derivatives with respect to the parameter λ_j , which are defined implicitly by the relations

$$2\partial_{\lambda_j} \rho(\lambda) = \rho(\lambda) \mathcal{L}_j + \mathcal{L}_j \rho(\lambda), \quad (5)$$

where we have used the notation $\partial_{\lambda_j} \equiv \partial/\partial\lambda_j$ for $j = 1, 2$. The QFIM provides a matrix lower bound on the average mean-square error (MSE) matrix of the estimates, usually

referred to as the multiparameter quantum Cramér-Rao bound (QCRB)

$$\mathbf{V}(\hat{\lambda}; \lambda) \geq \frac{1}{M\mathcal{F}(\lambda)}, \quad (6)$$

where $\mathbf{V}(\hat{\lambda}; \lambda)$ is the covariance matrix of λ , M the number of independently repeated measurements.

If we now introduce the $d \times d$ real, weight matrix W (can be any semidefinite matrix), we may obtain a useful scalar bound as

$$\text{Tr}[\mathbf{W}\mathbf{V}(\hat{\lambda}, \lambda)] \geq \text{Tr}[\mathbf{W}M\mathcal{F}^{-1}(\lambda)] = C_S(\mathbf{W}, \lambda), \quad (7)$$

which is usually referred to as the SLD-QFI scalar bound, and represents a benchmark for multiparameter estimation. The SLD-QCRB is generally not attainable, due to the incompatibility of generators of different parameters, which is reflected by the noncommutativity of the corresponding SLDs. Indeed, the optimal measurement operators corresponding to the different parameters may not commute with each other, making this scalar bound unreachable. The SLD-QCRB is achievable if the Uhlmann curvature matrix with elements [27–29]

$$[\mathcal{U}(\lambda)]_{nm} = -\frac{i}{2} \text{Tr}[\rho(\lambda) [\mathcal{L}_n, \mathcal{L}_m]] \quad (8)$$

vanishes. We recall that multiparameter quantum metrology corresponds to simultaneous estimation of multiple parameters using a single quantum system to probe a quantum dynamics with unknown parameters. In other words, if one wishes to estimate separate parameters as precisely as one would estimate them individually when assuming perfect knowledge of the other parameters, then compatibility conditions need to be satisfied, which is precisely the vanishing of the Uhlmann curvature matrix $\mathcal{U}(\lambda) = \mathbf{0}$. This ensures the existence of compatible measurements and the possibility of saturating the SLD-QCRB. In addition, there must exist a single probe state $\rho(\lambda)$ leading to the optimal QFI for each of the parameters under consideration.

In our case, we have two parameters χ and γ and the corresponding SLDs are defined implicitly (at any time) by

$$2\partial_\chi \rho(\lambda) = \rho(\lambda) \mathcal{L}_\chi + \mathcal{L}_\chi \rho(\lambda), \quad (9)$$

$$2\partial_\gamma \rho(\lambda) = \rho(\lambda) \mathcal{L}_\gamma + \mathcal{L}_\gamma \rho(\lambda). \quad (10)$$

In order to evaluate the QFIM and the Uhlmann matrix at any time we write the derivatives of the master equation (2) with respect to the parameters χ and γ and obtain

$$\begin{aligned} \frac{d}{dt} \partial_\chi \rho(\lambda) &= -i[\hat{H}, \partial_\chi \rho(\lambda)] - i[\partial_\chi \hat{H}, \rho(\lambda)] \\ &\quad + \frac{\gamma}{2} \mathcal{D}[\hat{a}] \partial_\chi \rho(\lambda) \equiv \partial_\chi (\mathcal{L}_0 \rho(\lambda)), \\ \frac{d}{dt} \partial_\gamma \rho(\lambda) &= -i[\hat{H}, \partial_\gamma \rho(\lambda)] + \frac{1}{2} \mathcal{D}[\hat{a}] \rho(\lambda) \\ &\quad + \frac{\gamma}{2} \mathcal{D}[\hat{a}] \partial_\gamma \rho(\lambda) \equiv \partial_\gamma (\mathcal{L}_0 \rho(\lambda)), \end{aligned} \quad (11)$$

where we have used the notation $\partial_k \equiv \partial/\partial k$ for $k = \chi, \lambda$. The above set of equations, together with the master equation (2), can be written in a compact matrix form as $\dot{\mathcal{R}}(t) = A\mathcal{R}(t)$,

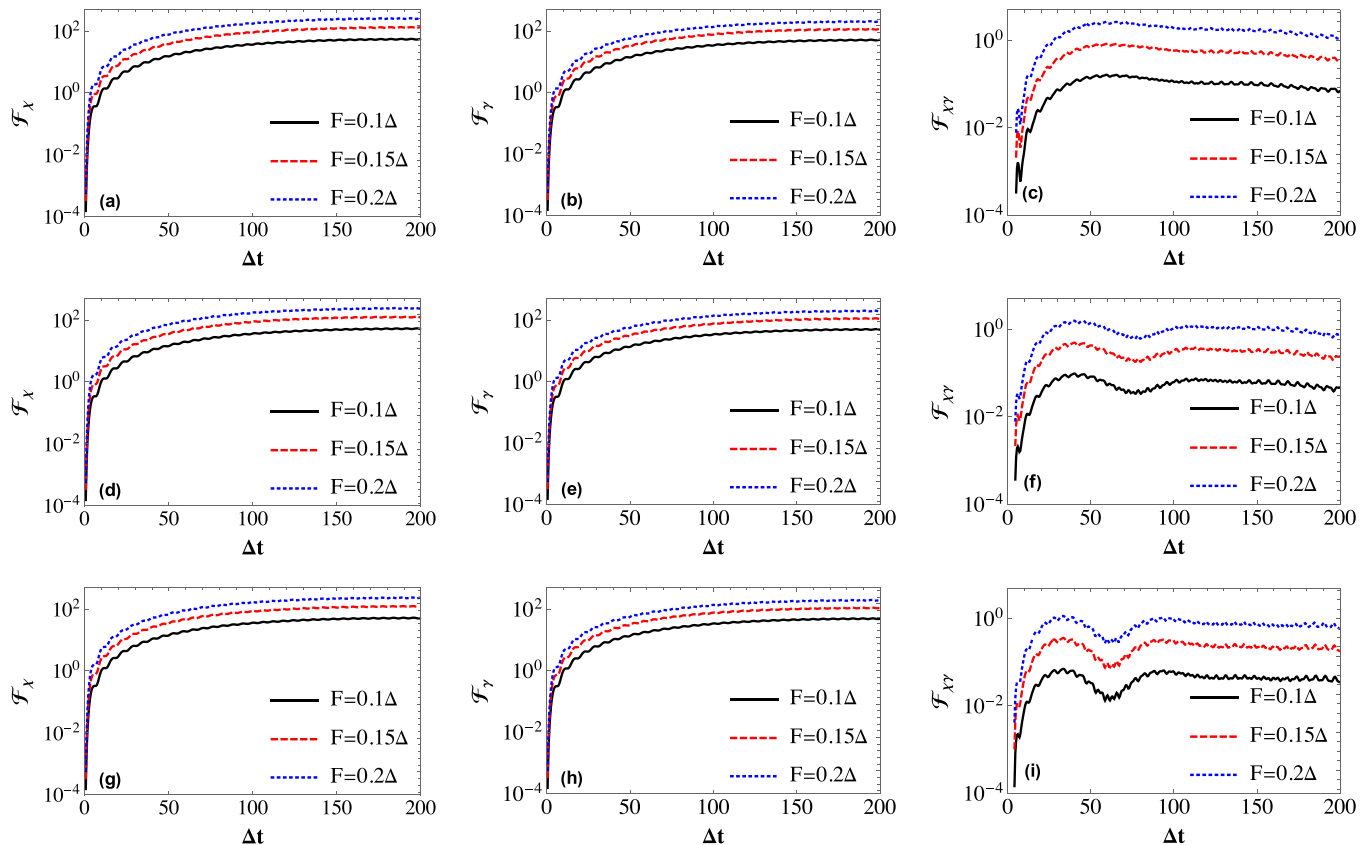


FIG. 1. The quantum Fisher information matrix elements as a functions of (renormalized) evolution time Δt . The first column shows results for \mathcal{F}_χ , the second one for \mathcal{F}_γ , and the last one shows the off-diagonal element of the QFIM $\mathcal{F}_{\chi\gamma}$. Parameters are set to $\chi = 0.1\Delta$ (first row), $\chi = 0.5\Delta$ (second row), and $\chi = \Delta$ (third row) and the different curves refer to different values of the driving strength $F = 0.1\Delta$ (black curves), $F = 0.2\Delta$ (blue curves), and $F = 0.15\Delta$ (red curves). We also set $\gamma = 0.01\Delta$.

where $\mathcal{R}(t) = [\rho(\lambda), \partial_\chi \rho(\lambda), \partial_\gamma \rho(\lambda)]^T$ and \mathcal{A} takes the form

$$\mathcal{A} = \begin{pmatrix} \mathcal{L}_0 & 0 & 0 \\ \partial_\chi \mathcal{L}_0 & \mathcal{L}_0 & 0 \\ \partial_\gamma \mathcal{L}_0 & 0 & \mathcal{L}_0 \end{pmatrix}. \quad (12)$$

We end this section by reminding that if the Uhlmann curvature vanishes, then it makes sense to address single-parameter estimation. In this case the relevant CR bounds are given by

$$\text{Var}\lambda \geq \frac{1}{M\mathcal{F}_{\lambda\lambda}}, \quad (13)$$

where $\lambda = \chi, \gamma$, Var denotes the variance of any unbiased estimator, and the quantities $\mathcal{F}_{\lambda\lambda}$ are the diagonal elements of the QFIM. These elements also provide bounds to the classical Fisher information of any observable aimed at estimating the parameter λ as follows. If we perform a measurement described by the probability operator-valued measure (POVM) $\{\Pi_x\}$, with $\sum \Pi_x = \mathbb{I}$, and obtain the distribution of outcomes $p(x|\lambda) = \text{Tr}[\rho(\lambda)\Pi_x]$, then we have $\mathcal{F}_X(\lambda) \leq \mathcal{F}_{\lambda\lambda}$ where $\mathcal{F}_X(\lambda) = \sum_x [\partial_\lambda p(x|\lambda)]^2 / p(x|\lambda)$ is the Fisher information of $p(x|\lambda)$, i.e., the maximum information about λ that may be extracted by measuring $\{\Pi_x\}$.

III. RESULTS

A. Elements of the QFIM and the Uhlmann curvature

Upon solving the system of coupled differential equations in (12), we may obtain the SLDs for the two parameters χ and γ and, in turn, the QFIM. In general, it is challenging to obtain symmetric logarithmic derivative $\mathcal{L}_{\chi,\gamma}$ analytically. In our case, we solve the above set of equations numerically to obtain the SLDs and then QFIM using the Python library QUTIP [80]. In doing this, we are free to tune the value of the driving F and the detuning Δ since these degrees of freedom are typically available in realistic situations. In particular, we evaluate the elements of the QFIM as a function of the renormalized interaction time Δt (since varying Δ simply corresponds to a change of the overall timescale) and for different values of the driving.

In Figs. 1(a)–1(c), we show the typical behavior of the QFI elements as a function of Δt for different values of the coherent drive strength F . The specific values used for these plots are $\chi = 0.1\Delta$ and $\gamma = 0.01\Delta$. We use the notation $\mathcal{F}_\lambda \equiv \mathcal{F}_{\lambda\lambda}$ for the diagonal elements of the QFIM, $\lambda = \chi, \gamma$ and $\mathcal{F}_{\chi\gamma}$ for the off-diagonal one. For small times, all the elements of the QFIM increase quite rapidly and then tend to saturate, at least in the range of interaction times we have explored numerically. Notice that our system is known to possess a stationary state [81], and this corroborates our findings,

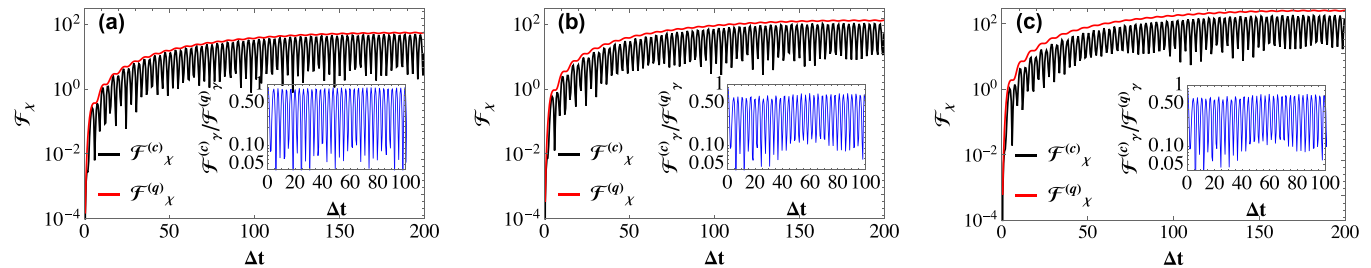


FIG. 2. Homodyne Fisher information $\mathcal{F}_X(\chi)$ for the nonlinearity as function of the rescaled time Δt for $F = 0.1\Delta$ (a), $F = 0.15\Delta$ (b), and $F = 0.2\Delta$ (c) for fixed value of $\chi = 0.05\Delta$. The corresponding diagonal element of the QFIM \mathcal{F}_X is shown for comparison. The insets show the ratio $\mathcal{F}_X(\chi)/\mathcal{F}_X$. The other parameters are set as in Fig. 1.

indicating the saturation of the values of the elements of the QFIM.

The off-diagonal term of the QFIM is nearly zero in all the conditions we have investigated numerically and, in turn, the Uhlmann curvature vanishes. This means that the loss and nonlinearity parameters may be jointly estimated, and no additional noise of quantum origin occurs in inferring them from measured data.

The diagonal terms of the QFIM govern the ultimate precision achievable in estimating χ and γ . Both elements increase with time and the amplitude of the coherent driving. A similar behavior may be observed for other values of the parameters. Overall, we conclude that joint estimation of loss and nonlinearity is possible, and to maximize precision one has to employ a moderately large driving (in unit of Δ) and a large interaction time ($\Delta t \sim 100$).

B. Estimation in practice: Performance of homodyne detection

In this section, we analyze the performance of homodyne detection, i.e., we evaluate the classical Fisher information of this detection scheme for one of the parameters and compare its value with the corresponding (diagonal) element of the QFIM. Homodyne detection measures a quadrature of the field, i.e., the Hermitian operator

$$x_\theta = \frac{1}{2}(ae^{-i\theta} + a^\dagger e^{i\theta}). \quad (14)$$

In our case, we set θ to zero. The POVM of the detector is given by $\Pi_x = |x\rangle\langle x|$ where, in the Fock representation, $|x\rangle$ is

given by

$$|x\rangle = \frac{1}{\pi^{1/4}} \sum_n \frac{\exp(-x^2/2)}{2^{n/2}(n!)^{1/2}} H_n(x) |n\rangle, \quad (15)$$

where $H_n(x)$ is the Hermite polynomial of order n . Since the quadrature has a continuous spectrum, the classical Fisher information is given by

$$\mathcal{F}_X(\lambda) = \int dx \frac{1}{p(x|\lambda)} \left[\frac{\partial p(x|\lambda)}{\partial \lambda} \right]^2, \quad (16)$$

where $p(x|\lambda) = \text{Tr}[\rho(\lambda) \Pi_x]$.

By using the numerical solution of the master equation (2), we evaluate the distribution $p(x|\chi, \gamma)$ at any time and, in turn, the two classical Fisher informations $\mathcal{F}_X(\chi)$ and $\mathcal{F}_X(\gamma)$. Results are illustrated in Figs. 2 and 3.

In Figs. 2(a)–2(c), we show $\mathcal{F}_X(\chi)$ as a function of the rescaled time Δt together with the QFIM element \mathcal{F}_X for $\chi = 0.05\Delta$ and different values of the driving amplitude F . As it is apparent from the plots, the homodyne Fisher information oscillates in time, with the maxima being very close to \mathcal{F}_X . In other words, homodyne detection provides a nearly optimal estimation scheme for the nonlinearity, though an accurate selection of the measurement time is required. In the insets of Figs. 2(a)–2(c), we show the ratio $\mathcal{F}_X(\chi)/\mathcal{F}_X$, which confirms the observations made above. Notice that both $\mathcal{F}_X(\chi)$ and \mathcal{F}_X increase with the amplitude of the coherent driving F .

Figures 3(a)–3(c) contain results similar to those in Figs. 2(a)–2(c), but for the loss parameter γ , i.e., $\mathcal{F}_X(\gamma)$ as a function of the rescaled time Δt together with the QFIM element \mathcal{F}_X for $\gamma = 0.01\Delta$ and different values of the driving amplitude F . Also for the loss parameter, the homodyne

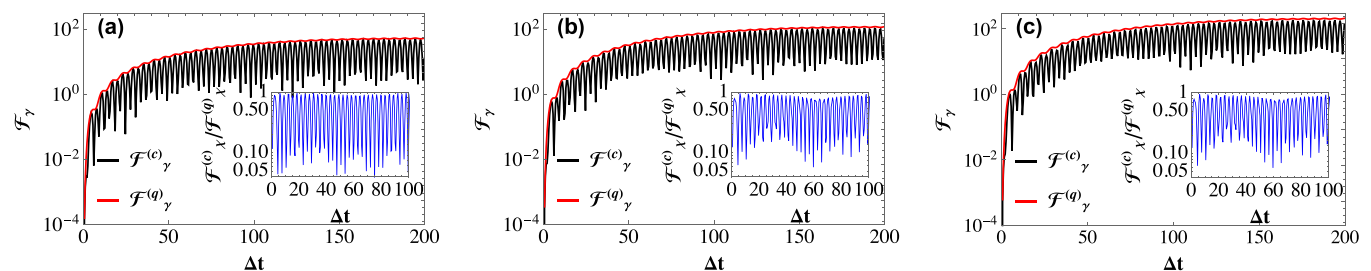


FIG. 3. Homodyne Fisher information $\mathcal{F}_X(\gamma)$ for the loss as function of the rescaled time Δt for $F = 0.1\Delta$ (a), $F = 0.15\Delta$ (b), and $F = 0.2\Delta$ (c) for fixed value of $\gamma = 0.01\Delta$. The corresponding diagonal element of the QFIM \mathcal{F}_X is shown for comparison. The insets show the ratio $\mathcal{F}_X(\gamma)/\mathcal{F}_X$. The other parameters are set as in Fig. 1.

Fisher information oscillates in time, with the maxima being very close to \mathcal{F}_γ , i.e., homodyne detection is a nearly optimal estimation scheme [82] provided that an accurate selection of the measurement time is available. In the insets, we show the ratio $\mathcal{F}_X(\gamma)/\mathcal{F}_\gamma$.

Notice that by changing the phase of the measured quadrature, we may change the position of the maxima of the homodyne Fisher information, i.e., a feedback mechanism may be used to achieve optimality.

IV. CONCLUSIONS

In this paper, we have addressed the joint estimation of loss and nonlinearity in driven-dissipative Kerr resonators, i.e., coherently driven Kerr oscillators in the presence of loss. In particular, we have considered the realistic situation in which the loss rate and the nonlinear coupling are the parameters of interest, whereas the amplitude of the coherent driving, and the detuning, are known and externally tunable.

Our results show that this driven-dissipative model is asymptotically classical, i.e., the Uhlmann curvature vanishes, and the two parameters may be jointly estimated without any additional noise of quantum origin. We have also found that

the ultimate precision, as quantified by the quantum Fisher information (QFI), may be improved, for both parameters, by increasing the interaction time and the driving amplitude.

Finally, we have investigated the performance of quadrature measurements, i.e., homodyne detection, and have shown that for both parameters homodyne Fisher information oscillates in time, repeatedly approaching the corresponding QFI. In other words, homodyne detection provides a nearly optimal estimation scheme for both loss and nonlinearity, though an accurate selection of the measurement time is required in both cases.

Our results show that driven-dissipative Kerr resonators are convenient probes for jointly estimating nonlinearity and loss without additional quantum noise, and pave the way for the experimental implementation in quantum optical systems.

ACKNOWLEDGMENTS

This work has been supported by Khalifa University of Science and Technology under Award No. 8474000358 (FSU-2021-018) (Estimation of Nonlinearities in Optical Media). This work was done under the auspices of INdAM-GNFM. M.G.A.P. thanks R. F. Antoni for motivating comments.

-
- [1] V. Giovannetti, S. Lloyd, and L. Maccone, *Quantum Metrology*, *Phys. Rev. Lett.* **96**, 010401 (2006).
 - [2] M. G. A. Paris, *Quantum estimation for quantum technology*, *Int. J. Quantum Inf.* **07**, 125 (2009).
 - [3] C. L. Degen, F. Reinhard, and P. Cappellaro, *Quantum sensing*, *Rev. Mod. Phys.* **89**, 035002 (2017).
 - [4] S. Pirandola, B. R. Bardhan, T. Gehring, C. Weedbrook, and S. Lloyd, *Advances in photonic quantum sensing*, *Nat. Photonics* **12**, 724 (2018).
 - [5] F. Troiani and M. G. A. Paris, *Universal Quantum Magnetometry with Spin States at Equilibrium*, *Phys. Rev. Lett.* **120**, 260503 (2018).
 - [6] M. Bina, F. Grasselli, and M. G. A. Paris, *Continuous-variable quantum probes for structured environments*, *Phys. Rev. A* **97**, 012125 (2018).
 - [7] F. S. Sehdaran, M. Bina, C. Benedetti, and M. G. A. Paris, *Quantum probes for ohmic environments at thermal equilibrium*, *Entropy* **21**, 486 (2019).
 - [8] F. Gebbia, C. Benedetti, F. Benatti, R. Floreanini, M. Bina, and M. G. A. Paris, *Two-qubit quantum probes for the temperature of an Ohmic environment*, *Phys. Rev. A* **101**, 032112 (2020).
 - [9] A. Candeloro, C. Degli Esposti Boschi, and M. G. A. Paris, *Quantum probes for universal gravity corrections*, *Phys. Rev. D* **102**, 056012 (2020).
 - [10] C. Benedetti and M. G. A. Paris, *Characterization of classical Gaussian processes using quantum probes*, *Phys. Lett. A* **378**, 2495 (2014).
 - [11] M. G. A. Paris, *Quantum probes for fractional Gaussian processes*, *Physica A* **413**, 256 (2014).
 - [12] Y. Sung, F. Beaudoin, L. M. Norris, F. Yan, D. K. Kim, J. Y. Qiu, U. von Lüpke, J. L. Yoder, T. P. Orlando, L. Viola *et al.*, *Non-Gaussian noise spectroscopy with a superconducting qubit sensor*, *Nat. Commun.* **10**, 3715 (2019).
 - [13] B. Gong, D. Dong, and W. Cui, *Weak-force sensing in optomechanical systems with Kalman filtering*, *J. Phys. A: Math. Theor.* **54**, 165301 (2021).
 - [14] E. Marchiori *et al.*, *Nanoscale magnetic field imaging for 2D materials*, *Nat. Rev. Phys.* **4**, 49 (2022).
 - [15] L. Thiel *et al.*, *Probing magnetism in 2D materials at the nanoscale with single-spin microscopy*, *Science* **364**, 973 (2019).
 - [16] K. Y. Yip *et al.*, *Measuring magnetic field texture in correlated electron systems under extreme conditions*, *Science* **366**, 1355 (2019).
 - [17] M. Lesik *et al.*, *Magnetic measurements on micrometer-sized samples under high pressure using designed NV centers*, *Science* **366**, 1359 (2019).
 - [18] S. Hsieh *et al.*, *Imaging stress and magnetism at high pressures using a nanoscale quantum sensor*, *Science* **366**, 1349 (2019).
 - [19] G. Kucsko *et al.*, *Nanometre-scale thermometry in a living cell*, *Nature (London)* **500**, 54 (2013).
 - [20] J. Choi *et al.*, *Probing and manipulating embryogenesis via nanoscale thermometry and temperature control*, *Proc. Natl. Acad. Sci. USA* **117**, 14636 (2020).
 - [21] C. Li, R. Soleyman, M. Kohandel, and P. Cappellaro, *SARS-CoV-2 quantum sensor based on nitrogen-vacancy centers in diamond*, *Nano Lett.* **22**, 43 (2021).
 - [22] A. Marais *et al.*, *The future of quantum biology*, *J. R. Soc. Interface.* **15**, 20180640 (2018).
 - [23] J. Li, H. Z. Shen, W. Wang, and X. Yi, *Atom-modulated dynamic optical hysteresis in driven-dissipative systems*, *Phys. Rev. A* **104**, 013709 (2021).
 - [24] L. McCuller, C. Whittle, D. Ganapathy, K. Komori, M. Tse, A. Fernandez-Galiana, L. Barsotti, P. Fritschel, M. MacInnis, F. Matichard *et al.*, *Frequency-Dependent Squeezing for Advanced LIGO*, *Phys. Rev. Lett.* **124**, 171102 (2020).

- [25] B. P. Abbott *et al.* (LIGO Scientific Collaboration and Virgo Collaboration), Observation of Gravitational Waves from a Binary Black Hole Merger, *Phys. Rev. Lett.* **116**, 061102 (2016).
- [26] M. Szczykulska, T. Baumgratz, and A. Datta, Multi-parameter quantum metrology, *Adv. Phys. X* **1**, 621 (2016).
- [27] S. Pang and T. A. Brun, Quantum metrology for a general Hamiltonian parameter, *Phys. Rev. A* **90**, 022117 (2014).
- [28] A. Carollo, B. Spagnolo, and D. Valenti, Uhlmann curvature in dissipative phase transitions, *Sci. Rep.* **8**, 9852 (2018).
- [29] J. S. Sidhu and P. Kok, Quantum Fisher information for general spatial deformations of quantum emitters, [arXiv:1802.01601](https://arxiv.org/abs/1802.01601).
- [30] A. Carollo, B. Spagnolo, A. A. Dubkov, and D. Valenti, Erratum: On quantumness in multi-parameter quantum estimation (2019 J. Stat. Mech. 094010), *J. Stat. Mech.* (2020) 029902.
- [31] J. Liu, H. Yuan, X.-M. Lu, and X. Wang, Quantum Fisher information matrix and multiparameter estimation, *J. Phys. A: Math. Theor.* **53**, 023001 (2020).
- [32] F. Albarelli, M. Barbieri, M. G. Genoni, and I. Gianani, A perspective on multiparameter quantum metrology: From theoretical tools to applications in quantum imaging, *Phys. Lett. A* **384**, 126311 (2020).
- [33] S. Razavian, M. G. A. Paris, and M. G. Genoni, On the quantumness of multiparameter estimation problems for qubit systems, *Entropy* **22**, 1197 (2020).
- [34] E. Polino, M. Valeri, N. Spagnolo, and F. Sciarrino, Photonic quantum metrology, *AVS Quantum Sci.* **2**, 024703 (2020).
- [35] J. S. Sidhu and P. Kok, Geometric perspective on quantum parameter estimation, *AVS Quantum Sci.* **2**, 014701 (2020).
- [36] A. Candeloro, S. Razavian, M. Piccolini, B. Teklu, S. Olivares, and M. G. A. Paris, Quantum probes for the characterization of nonlinear media, *Entropy* **23**, 1353 (2021).
- [37] T. Heinosaari, T. Miyadera, and M. Ziman, An invitation to quantum incompatibility, *J. Phys. A: Math. Theor.* **49**, 123001 (2016).
- [38] S. Ragy, M. Jarzyna, and R. Demkowicz-Dobrzanski, Compatibility in multiparameter quantum metrology, *Phys. Rev. A* **94**, 052108 (2016).
- [39] F. Belliardo and V. Giovannetti, Incompatibility in quantum parameter estimation, *New J. Phys.* **23**, 063055 (2021).
- [40] J. S. Sidhu, Y. Ouyang, E. T. Campbell, and P. Kok, Tight Bounds on the Simultaneous Estimation of Incompatible Parameters, *Phys. Rev. X* **11**, 011028 (2021).
- [41] R. Chacón, General results on chaos suppression for biharmonically driven dissipative systems, *Phys. Lett. A* **257**, 293 (1999).
- [42] E. G. Dalla Torre, E. Demler, T. Giamarchi, and E. Altman, Dynamics and universality in noise-driven dissipative systems, *Phys. Rev. B* **85**, 184302 (2012).
- [43] L. Campos Venuti and P. Zanardi, Dynamical response theory for driven-dissipative quantum systems, *Phys. Rev. A* **93**, 032101 (2016).
- [44] P. Comaron, G. Dagvadorj, A. Zamora, I. Carusotto, N. P. Proukakis, and M. H. Szymańska, Dynamical Critical Exponents in Driven-Dissipative Quantum Systems, *Phys. Rev. Lett.* **121**, 095302 (2018).
- [45] B. Zhu, J. Marino, N. Y. Yao, M. D. Lukin, and E. A. Demler, Dicke time crystals in driven-dissipative quantum many-body systems, *New J. Phys.* **21**, 073028 (2019).
- [46] M. Soriente, R. Chitra, and O. Zilberberg, Distinguishing phases using the dynamical response of driven-dissipative light-matter systems, *Phys. Rev. A* **101**, 023823 (2020).
- [47] H. Landa, M. Schiró, and G. Misguich, Correlation-induced steady states and limit cycles in driven dissipative quantum systems, *Phys. Rev. B* **102**, 064301 (2020).
- [48] B. O. Goes and G. T. Landi, Entropy production dynamics in quench protocols of a driven-dissipative critical system, *Phys. Rev. A* **102**, 052202 (2020).
- [49] N. Chanda and R. Bhattacharyya, Emergence of the Born rule in strongly driven dissipative systems, *Phys. Rev. A* **104**, 022436 (2021).
- [50] Sh. Saedi and F. Kheirandish, Exact density matrix elements for a driven dissipative system described by a quadratic Hamiltonian, *Sci. Rep.* **11**, 17388 (2021).
- [51] G. Zhao, Y. Wang, and X.-F. Qian, Driven dissipative quantum dynamics in a cavity magnon-polariton system, *Phys. Rev. B* **104**, 134423 (2021).
- [52] L. R. Bakker, M. S. Bahoovadinov, D. V. Kurlov, V. Gritsev, A. K. Fedorov, and D. O. Krimer, Driven-Dissipative Time Crystalline Phases in a Two-Mode Bosonic System with Kerr Nonlinearity, *Phys. Rev. Lett.* **129**, 250401 (2022).
- [53] D. Dahan, G. Arwas, and E. Grosfeld, Classical and quantum chaos in chirally-driven, dissipative Bose-Hubbard systems, *npj Quantum Inf.* **8**, 14 (2022).
- [54] M. L. Olivera-Atencio, L. Lamata, S. Kohler, and J. Casado-Pascual, Universal patterns in multifrequency-driven dissipative systems, *Europhys. Lett.* **137**, 12001 (2022).
- [55] S. Shahidani and M. Rafiee, Irreversible entropy production rate in a parametrically driven-dissipative system: The role of self-correlation between noncommuting observables, *Phys. Rev. A* **105**, 052430 (2022).
- [56] H.-Y. Wang, X.-M. Zhao, L. Zhuang, and W.-M. Liu, Non-Floquet engineering in periodically driven dissipative open quantum systems, *J. Phys.: Condens. Matter* **34**, 365402 (2022).
- [57] P. D. Drummond and D. F. Walls, Quantum theory of optical bistability. I. Nonlinear polarisability model, *J. Phys. A: Math. Gen.* **13**, 725 (1980).
- [58] M. A. C. Rossi, F. Albarelli, and M. G. A. Paris, Enhanced estimation of loss in the presence of Kerr nonlinearity, *Phys. Rev. A* **93**, 053805 (2016).
- [59] V. Montenegro, A. Ferraro, and S. Bose, Nonlinearity-induced entanglement stability in a qubit-oscillator system, *Phys. Rev. A* **90**, 013829 (2014).
- [60] D. O. Krimer and M. Pletyukhov, Few-Mode Geometric Description of a Driven-Dissipative Phase Transition in an Open Quantum System, *Phys. Rev. Lett.* **123**, 110604 (2019).
- [61] V. Montenegro, M. G. Genoni, A. Bayat, and M. G. A. Paris, Probing of nonlinear hybrid optomechanical systems via partial accessibility, *Phys. Rev. Res.* **4**, 033036 (2022).
- [62] X. H. H. Zhang and H. U. Baranger, Driven-dissipative phase transition in a Kerr oscillator: From semiclassical \mathcal{PT} symmetry to quantum fluctuations, *Phys. Rev. A* **103**, 033711 (2021).
- [63] K. Sala, T. Doicin, A. D. Armour, and T. Tufarelli, Quantum estimation of coupling strengths in driven-dissipative optomechanics, *Phys. Rev. A* **104**, 033508 (2021).
- [64] X. Li, Y. Li, and J. Jin, Steady-state susceptibility in continuous phase transitions of dissipative systems, *Phys. Rev. A* **105**, 052226 (2022).

- [65] F. Bibak, U. Delić, M. Aspelmeyer, and B. Dakić, Dissipative phase transitions in optomechanical systems, [arXiv:2208.11964](#).
- [66] M. J. Kewming, M. T. Mitchison, and G. T. Landi, Diverging current fluctuations in critical Kerr resonators, *Phys. Rev. A* **106**, 033707 (2022).
- [67] D. Xie, C. Xu, and A. M. Wang, Quantum estimation of Kerr nonlinearity in driven-dissipative systems, *Results Phys.* **42**, 105957 (2022).
- [68] L. M. Sieberer, M. Buchhold, and S. Diehl, Keldysh field theory for driven open quantum systems, *Rep. Prog. Phys.* **79**, 096001 (2016).
- [69] I. Rotter and J. P. Bird, A review of progress in the physics of open quantum systems: theory and experiment, *Rep. Prog. Phys.* **78**, 114001 (2015).
- [70] S. Dutta and N. Cooper, Critical Response of a Quantum van der Pol Oscillator, *Phys. Rev. Lett.* **123**, 250401 (2019).
- [71] A. V. Kavokin, J. J. Baumberg, G. Malpuech, and F. P. Laussy, *Microcavities* (Oxford University Press, New York, 2007).
- [72] S. R. K. Rodriguez *et al.*, Probing a Dissipative Phase Transition via Dynamical Optical Hysteresis, *Phys. Rev. Lett.* **118**, 247402 (2017).
- [73] T. Fink *et al.*, Signatures of a dissipative phase transition in photon correlation measurements, *Nat. Phys.* **14**, 365 (2018).
- [74] Z. Geng, K. J. H. Peters, A. A. P. Trichet, K. Malmir, R. Kolkowski, J. M. Smith, and S. R. K. Rodriguez, Universal Scaling in the Dynamic Hysteresis, and Non-Markovian Dynamics, of a Tunable Optical Cavity, *Phys. Rev. Lett.* **124**, 153603 (2020).
- [75] P. Brookes *et al.*, Critical slowing down in circuit quantum electrodynamics, *Sci. Adv.* **7**, eabe9492 (2021).
- [76] Z. Leghtas *et al.*, Quantum engineering. Confining the state of light to a quantum manifold by engineered two-photon loss, *Science* **347**, 853 (2015).
- [77] A. Blais, A. L. Grimsmo, S. M. Girvin, and A. Wallraff, Circuit quantum electrodynamics, *Rev. Mod. Phys.* **93**, 025005 (2021).
- [78] J. Mendoza-Arenas, S. R. Clark, S. Felicetti, G. Romero, E. Solano, D. G. Angelakis, and D. Jaksch, Beyond mean-field bistability in driven-dissipative lattices: Bunching-antibunching transition and quantum simulation, *Phys. Rev. A* **93**, 023821 (2016).
- [79] C. Sánchez Muñoz, A. Lara, J. Puebla, and F. Nori, Hybrid Systems for the Generation of Nonclassical Mechanical States via Quadratic Interactions, *Phys. Rev. Lett.* **121**, 123604 (2018).
- [80] J. R. Johansson, P. D. Nation, and F. Nori, QuTiP 2: A Python framework for the dynamics of open quantum systems, *Comput. Phys. Commun.* **184**, 1234 (2013).
- [81] N. Bartolo, F. Minganti, W. Casteels, and C. Ciuti, Exact steady state of a Kerr resonator with one- and two-photon driving and dissipation: Controllable Wigner-function multimodality and dissipative phase transitions, *Phys. Rev. A* **94**, 033841 (2016).
- [82] G. Mauro D'Ariano, M. G. A. Paris, and M. F. Sacchi, Parameter estimation in quantum optics, *Phys. Rev. A* **62**, 023815 (2000).